Growth mechanisms and defect structures of $B_{12}As_2$ epilayers grown on 4H-SiC substrates

Yu Zhang, Hui Chen, Michael Dudley, Yi Zhang, J. H. Edgar, Yinyan Gong, Silvia Bakalova, Martin Kuball, Lihua Zhang, Dong Su, Yimei Zhu

How to cite this manuscript

Published Version Information

Growth Mechanisms and Defect Structures of $B_{12}As_2$ Epilayers Grown on 4H-SiC Substrates

Yu Zhang[1], Hui Chen[1], Michael Dudley[1], Yi Zhang[2], J. H. Edgar[2], Yinyan Gong[3], Silvia Bakalova[3], Martin Kuball[3], Lihua Zhang[4], Dong Su[4], Yimei Zhu[4]

[1]*Department of Materials Science and Engineering, Stony Brook University, Stony Brook, NY, 11794-2275, U.S.A.*

[2]*Department of Chemical Engineering, Kansas State University, Manhattan, KS 66506, U.S.A.*

[3]*H.H. Wills Physics Laboratory, University of Bristol, Bristol, United Kingdom*

[4]*Center for Functional Materials, Brookhaven National Laboratory, Upton, NY 11973-5000, U.S.A.*

Corresponding author: Prof. Michael Dudley

Phone: 631-632-8500   Fax: 631-632-8052   Email: mdudley@notes.cc.sunysb.edu

ABSTRACT

Epitaxial growth of icosahedral $B_{12}As_2$ on c-plane 4H-SiC substrates has been analyzed. On on-axis c-plane 4H-SiC substrates, Synchrotron white beam x-ray topography (SWBXT) revealed the presence of a homogenous solid solution of twin and matrix $B_{12}As_2$ epilayer domains. High resolution transmission electron microscopy (HRTEM) and scanning transmission electron microscopy (STEM) both revealed the presence of an ~20nm thick, disordered transition layer at the interface. (0003) twin boundaries are shown to possess fault vectors such as $1/3[1\text{-}100]_{B12As2}$ which originate from the mutual shift between the nucleation sites. On the contrary, $B_{12}As_2$ epilayers grown on c-plane 4H-SiC substrates intentionally misoriented from (0001) towards [1-100] is shown to be free of rotational twinning. SWBXT, HRTEM and STEM all confirmed the single crystalline nature and much higher quality of the films. In addition, no intermediate layer between the epilayer and the substrate was observed.

It is proposed that the vicinal steps formed by hydrogen etching on the off-axis 4H-SiC substrate surface before deposition cause the film to adopt a single orientation during nucleation process. This work also demonstrates that c-plane 4H-SiC with offcut toward [1-100] is potentially a good substrate choice for the growth of high-quality, single crystalline $B_{12}As_2$ epilayers for future device applications.

KEYWORDS

A1.Characterization; A1.Defects; A1.X-ray topography; A3.Heteroepitaxy Growth

INTRODUCTION

$B_{12}As_2$ is an important member of the icosahedral boride family of materials based on icosahedral clusters of boron atoms and two-atom As-As chains lying along the rhombohedral [111] axis. With a wide band gap of 3.2eV [1][2] at room temperature, it possesses exceptional radiation resistance mediated via "self-healing" mechanism which makes it an ideal choice for applications in high radiation environments [3]-[8], such as high-power beta-voltaic cells which are able to convert nuclear energy into electrical power at high efficiency [9][10]. Furthermore, $B_{12}As_2$ has high melting point, extraordinary mechanical properties and much larger Seebeck coefficient at high temperatures compared to conventional semiconductors which make it attractive for the development and fabrication of high temperature thermoelectronics [11][12]. Lastly, with the extraordinary neutron-absorbing ability of the $_{10}B$ isotope, $B_{12}As_2$ has also attracted considerable attention as a potential material for the fabrication of compact solid-state neutron detectors [12][13].

The absence of native substrates makes the growth of $B_{12}As_2$ via heteroepitaxy on non-native substrates with compatible structural parameters necessary. Hexagonal phases of SiC (a=3.08Å), such as 6H-SiC, have been the substrates of choice since they have approximately half of the basal plane lattice constant of $B_{12}As_2$ (a=6.14Å) [14][15][16]. However, growth of a lower symmetry epilayer on a higher symmetry substrate always produces structural variants (rotational and translational) in the film that are related to each other by a symmetry operation that is present in the substrate but absent in the epilayer, which

has been referred to the phenomenon as degenerate epitaxy [17][18]. Therefore, high densities of twin boundaries were observed in $B_{12}As_2$ epilayers grown on the substrates attempted so far [14][15]. However, twinning in $B_{12}As_2$ is expected to have a detrimental effect on device performance which has severely hindered development of this material to date. The elimination of twinning in $B_{12}As_2$ has become a primary goal for the $B_{12}As_2$ crystal growth community. It has been proposed that m-plane 15R-SiC is potentially a good substrate choice for the growth of untwined $B_{12}As_2$ epilayers [19]. However, because of the limited resource of pure 15R-SiC substrates, it is very important to discover other good substrates which are commercial-available. Therefore, we have explored the use of commercially available 4H-SiC substrates both on-axis and with particular offcut direction to explore the possibility to manipulate the relative populations of the multiple variants. High quality single crystalline $B_{12}As_2$ epilayers were achieved on 4H-SiC substrates intentionally misoriented from (0001) towards [1-100] and the growth mechanisms were proposed. Defect structures of twinned $B_{12}As_2$ epilayers grown on on-axis 4H-SiC substrates were also investigated. The goals of the studies are to understand the growth mechanisms and defect structures present in $B_{12}As_2$ epitaxial films so as to develop strategies to reduce defect densities, obtain single crystalline epilayers and better film quality for future device fabrications.

EXPERIMENT

$B_{12}As_2$ was deposited using chemical vapor deposition (CVD) method onto hydrogen-etched c-plane 4H-SiC substrates at 1350°C and 100 Torr of reactor pressure for 2 hours, using 1% B_2H_6 in H_2 and 1% AsH_3 in H_2 as sources. The epitaxial $B_{12}As_2$ films had a nominal thickness of around 4 µm. The film/substrate orientations were determined on as-grown films by SWBXT at the Stony Brook synchrotron topography facility at the National Synchrotron Light Source. The cross-sectional TEM samples were prepared parallel to (11-20)$_{4H-SiC}$, which is parallel to (11-20)$_{B12As2}$, since this orientation clearly reveals the $B_{12}As_2$ twin boundaries. Atomic structure of the film/substrate interface and the epilayer was examined by HRTEM using a JEOL 2100 system with an electron voltage of 200keV and

STEM using a Hitachi HD 2700C system at Brookhaven National Laboratory.

RESULTS AND DISCUSSION

Fig 1 (a) Shows a transmission synchrotron x-ray Laue pattern from a $B_{12}As_2$ epitaxial layer grown on an on-axis c-plane 4H-SiC substrate. The $B_{12}As_2$ produced weak and diffused diffraction spots that indicates the existence of mosaicity. Detailed analysis of diffraction pattern index not only shows the expected epitaxial relationship as $(0001)_{B12As2}<1-100>_{B12As2}||(0001)_{4H-SiC}<1-100>_{4H-SiC}$, but also confirms that the $B_{12}As_2$ is present in two distinct orientations which are related by a 180° (or equivalently 60°) rotation about the $(0001)_{B12As2}$ plane normal. This was corroborated with SEM observation (Fig 1 (b)) which reveals a composite structure comprising two types of equilateral triangular feature, each with dimensions of several µm, which are mutually rotated by 180° about the surface normal. These triangular grains correspond to twin related $B_{12}As_2$ domains. The morphology of the triangular features was determined using orientation information provided by SWBXT and found to consist of a flat $(0001)_{B12As2}$ facet bounded by three equivalent $(1-100)_{B12As2}$ facets. Further microstructural information, in particular concerning the boundaries between the various domains, was provided by HRTEM and STEM studies carried out on cross-sectional samples.

(a)   (b)

Fig 1 (a) Laue pattern of $B_{12}As_2$ on on-axis c-plane 4H-SiC with subscripts I and II showing diffraction spots from $B_{12}As_2$ matrix and twin; (b) SEM image of $B_{12}As_2$ film on on-axis c-plane 4H-SiC indicating $B_{12}As_2$ matrix and twin orientations.

High resolution cross-sectional TEM observation along the [11-20] zone axis (Fig 2(a)) reveals a transition layer located between the film and the substrate. Fig 2 (b) and (c) show selective area diffraction (SAD) patterns recorded from a local area in the $B_{12}As_2$ film and the 4H-SiC substrate respectively, confirming that the epilayer consists of an overlap of twinned $B_{12}As_2$ domains.
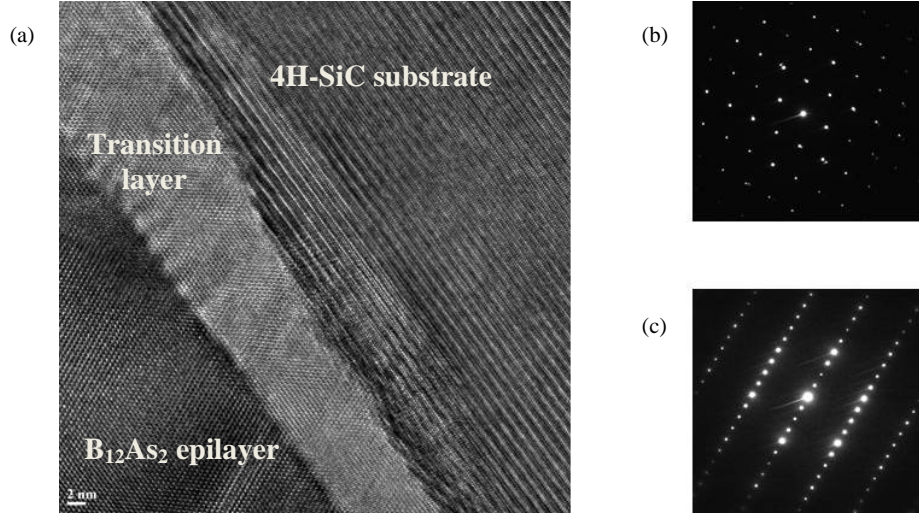

Fig 2 (a) Cross-sectional TEM image recorded along [11-20] revealing a transition layer located between the $B_{12}As_2$ layer and the 4H-SiC substrate. (b) SAD pattern of the $B_{12}As_2$ epilayer recorded along the [11-20] zone axis. (c) SAD pattern of the 4H-SiC substrate recorded along the [11-20] zone axis.

Fig 3 (a) shows a STEM image recorded from a region of the $B_{12}As_2$ film close to the interface containing an (0003) twin boundary. Fig 3 (b) is the magnified image of the boundary region in Fig 3 (a) which exhibits a shift of around 3.56Å, corresponding to $1/3[1-100]_{B12As2}$, thus confirming the formation mechanism. Such shifts were commonly observed in twin boundaries throughout the film. This type of twin boundary can be referred to as a "faulted twin boundary".
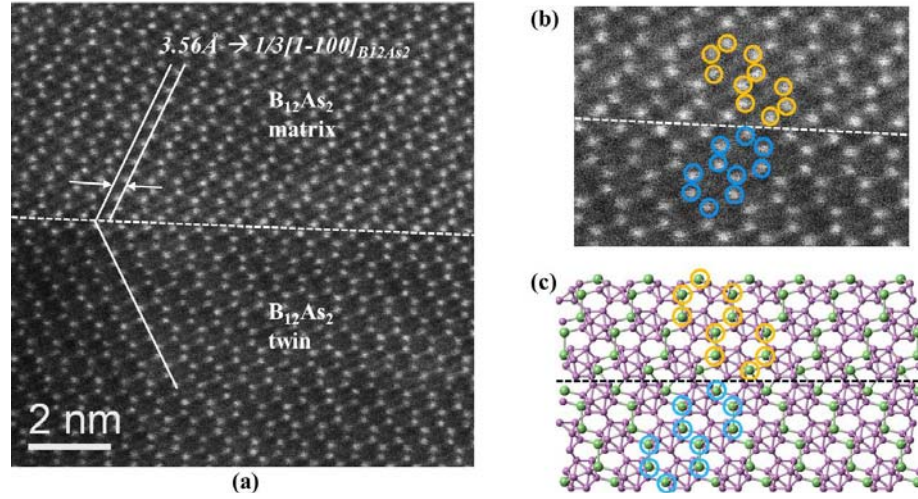
Fig 3 High resolution STEM image of the film ((a) and (b)) taken along [11-20] on on-axis c-plane 4H-SiC and corresponding crystal visualization ((c))showing the postulated atomic configuration across a $\{0003\}_{B12As2}$ twin boundary with $1/3 <1\text{-}100>_{B12As2}$ shift. The solid circles stand for the projection of columns comprising arsenic atoms.

In addition to providing information on the nucleation sites, STEM of the twin boundaries in comparison with CrystalMaker structural projections enables the possible bonding configurations across the observed (0003) twin boundaries to be assessed. For the faulted twin boundary exhibiting the $1/3[1\text{-}100]_{B12As2}$ shift, the structure proposed in Fig 3 (c) maintains reasonable bonding and agrees well with the STEM observations.

Fig 4(a) shows a transmission synchrotron x-ray Laue pattern from a $B_{12}As_2$ epitaxial layer grown on an off-axis c-plane 4H-SiC substrate with 7° offcut from (0001) toward [1-100] direction. The $B_{12}As_2$ produced much stronger and better-defined diffraction spots compared to previous results from $B_{12}As_2$ grown on other SiC substrates. Lower streaking indicated improved mosaicity and decreased strain level. The Laue pattern also lacked any evidence for the existence of twins, indicating the single crystalline nature of the $B_{12}As_2$. Detailed indexing analysis confirms the expected $(0001)_{B12As2}<1\text{-}100>_{B12As2}\|(0001)_{4H\text{-}SiC}<1\text{-}100>_{4H\text{-}SiC}$ in epitaxial relationship. The single crystalline nature and good epilayer quality observed via SWBXT was corroborated with SEM observations (Fig 4(b)) which reveals a relatively smooth and flat surface morphology when even lower voltage and higher magnification was employed in SEM.
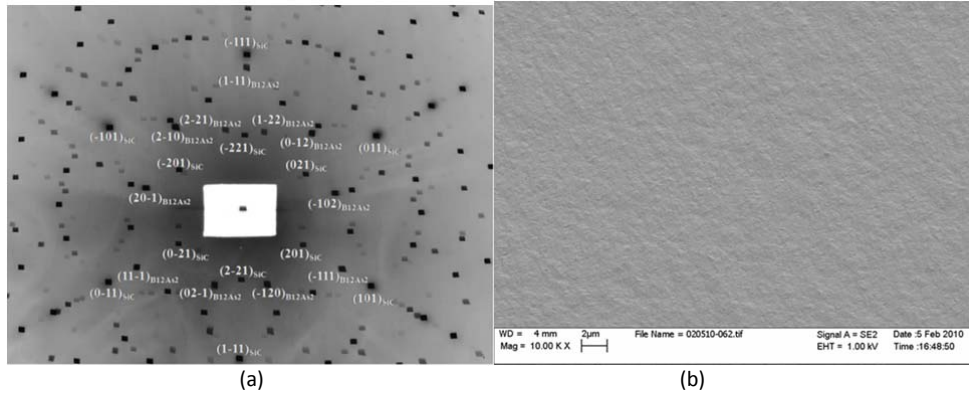
Fig 4 (a)SWBXT Laue pattern of single crystalline $B_{12}As_2$ on off-axis 4H-SiC, with the diffraction peaks marked with rhombohedral (hkl) indices.(b) SEM observation of $B_{12}As_2$ epilayer grown on off-axis 4H-SiC under lower voltage and higher magnification.

Excellent crystal quality and the elimination of degenerate epitaxy is also apparent in the HRTEM micrograph shown in Fig 5(a), which shows a strikingly abrupt, clean interface to the 4H-SiC substrate. SAD patterns from both 4H-SiC and $B_{12}As_2$ were also obtained (Fig 5(b) and (c)) in which the pattern from $B_{12}As_2$ shows clean diffractions from single orientation. The superior quality of the epilayer and the sharp interface without any transitional layer in between is observed using STEM at the film/substrate interface area (see Fig 6(a)). According to STEM observation, atomic modeling is generated showing only Si and As atoms which are the only heavy atoms visible under STEM (Fig 6(b)) and the complete atomic structure is shown in Fig 6 (c).
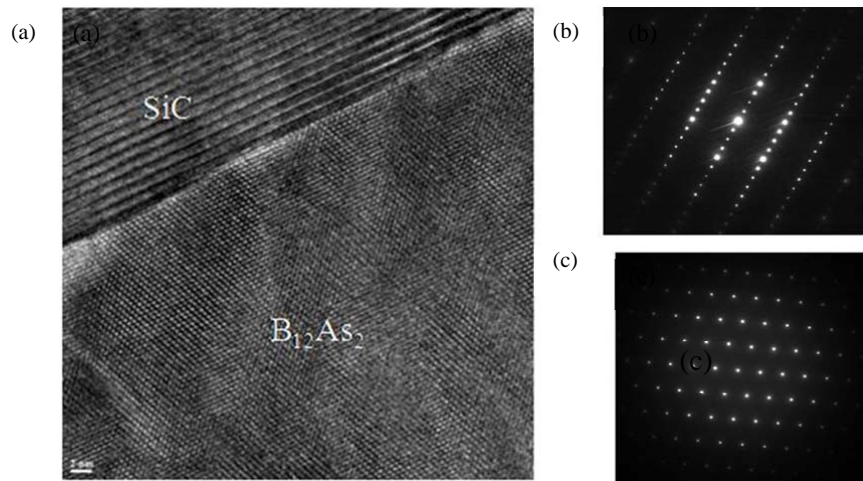

Fig 5 (a) HRTEM image taken along the [10-1] zone axis (equivalent to [11-20] in the hexagonal system) showing a sharp $B_{12}As_2$/off-axis 4H-SiC interface and perfect $B_{12}As_2$ single crystal; (b) SAD pattern of 4H-SiC substrate; (c) SAD pattern of $B_{12}As_2$ epilayer.
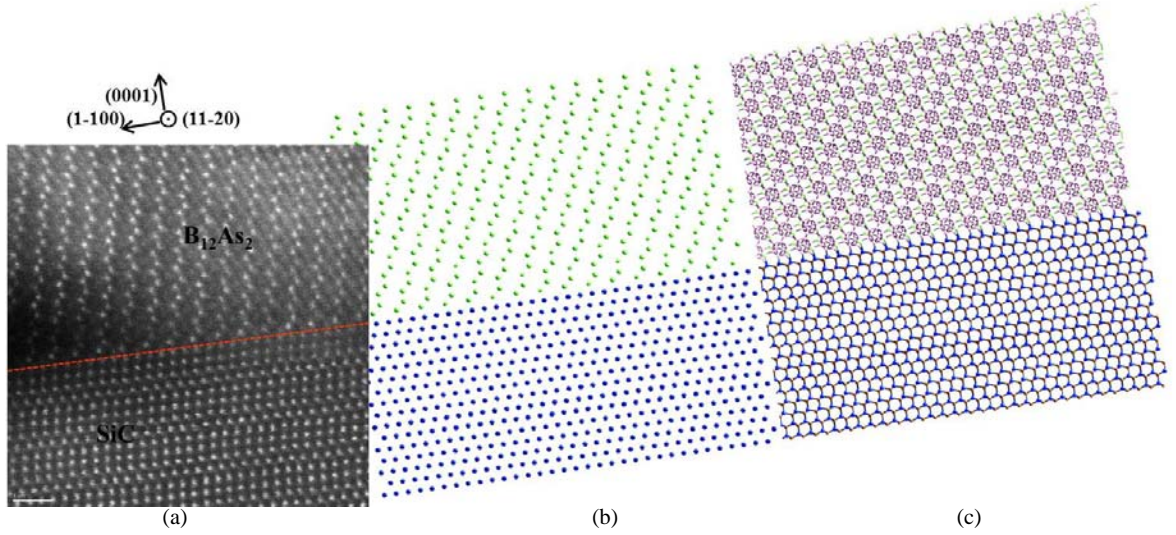
Fig 6 (a) STEM results along film/epilayer interface with [11-20] viewing direction on off-axis 4H-SiC showing the sharp and clear interface and no transitional layer in between. According to STEM observation, atomic modeling is generated showing only Si and As atoms which are the only atoms visible under STEM (b) and the complete atomic structure (c).

The significant improvement in microstructural quality achieved when using off-axis (0001) 4H-SiC substrates with specific [1-100] offcut direction can be understood by considering the step configurations expected to be exhibited on such substrates following hydrogen etching. These step configurations are known to comprise (0001) terraces and two kinds of single bilayer high (quarter-unit-cell-height) step risers; (-3304) which are close-packed and exhibit single dangling bonds and (-3308) which exhibit double dangling bonds. Both types of step risers have (0001) surface projections along <11-20> leading to relatively ordered step structures on samples offcut towards [1-100] (Fig 7). This can be contrasted with samples offcut towards [11-20] which will exhibit a much more disordered, zig-zag like step configuration (Fig 8 (a)).
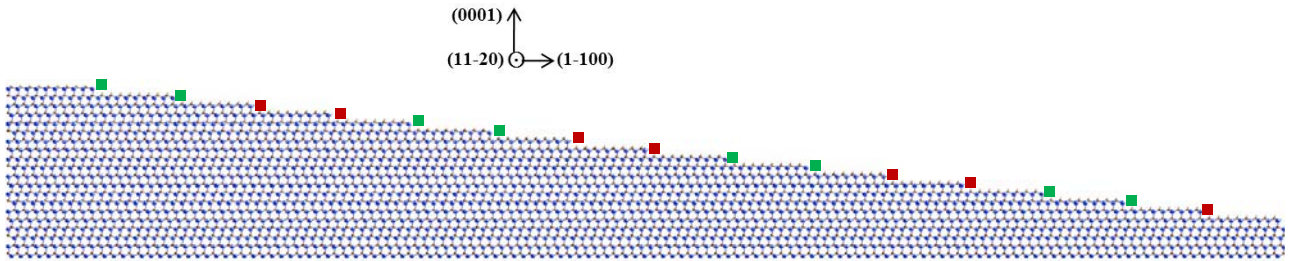

Fig 7 Step configuration created by hydrogen etching of the c-plane 4H-SiC substrate with 7° offcut toward [1-100] direction. Red labels (-3304) step risers and green labels (-3308) ones.

The evidence of surface morphology is shown in Fig 8 (b) in which an optical image is taken from the surface of a 4H-SiC boule. The spiral steps shown on the surface consist of two different types: (1-100) type which are ordered steps with straight step risers facing outward (labeled with orange arrows); (11-20) type which are disordered steps with irregular curved step risers facing outward (labeled with dotted blue arrows).

(a)   (b)

Fig 8 (a) Surface morphology of half unit cell height steps in 4H-SiC showing the orientations of the various step risers which have (0001) surface projections parallel to <11-20> (perpendicular to <1-100>); (b) Optical image of 4H-SiC boule showing surface morphology consisting of (1-100) type ordered step risers and (11-20) type disordered ones.

During hydrogen etching process, the step risers with double dangling bonds on the substrate surface will react with hydrogen and recede simultaneously at twice the velocity of those with single dangling bond. Step risers which are advancing backwards faster will eventually meet the next step riser which is advancing slower and will not be able to recede underneath the next step. Instead, they will slow down to the same receding speed as the next step riser which leads to the step bunching and the isolation of intersections between close packed (-3304) step risers and close packed (0001) terraces.

During the step flow growth process where $B_{12}As_2$ growth is subsequently carried out, $B_{12}As_2$ molecules that adsorb away from the step risers will generally only be able to weakly bond to the (0001) terraces from where they will most likely desorb. Considering the dangling bond configurations exhibited at the isolated intersections between the 1/4c height (-

3304) risers and the (0001) terraces on the substrate surface and the lattice geometry, $B_{12}As_2$ icosahedra are able to bond to both terrace and the adjacent step riser simultaneously and nucleate the growth process (Fig 9 (a) and (b)). Fig 9 (c) shows in plan-view that the triangular configuration of B atoms at the bottoms of B icosahedra bond to the similarly oriented triangular configurations of C atoms exposed on the (0001) 4H-SiC terrace. This can
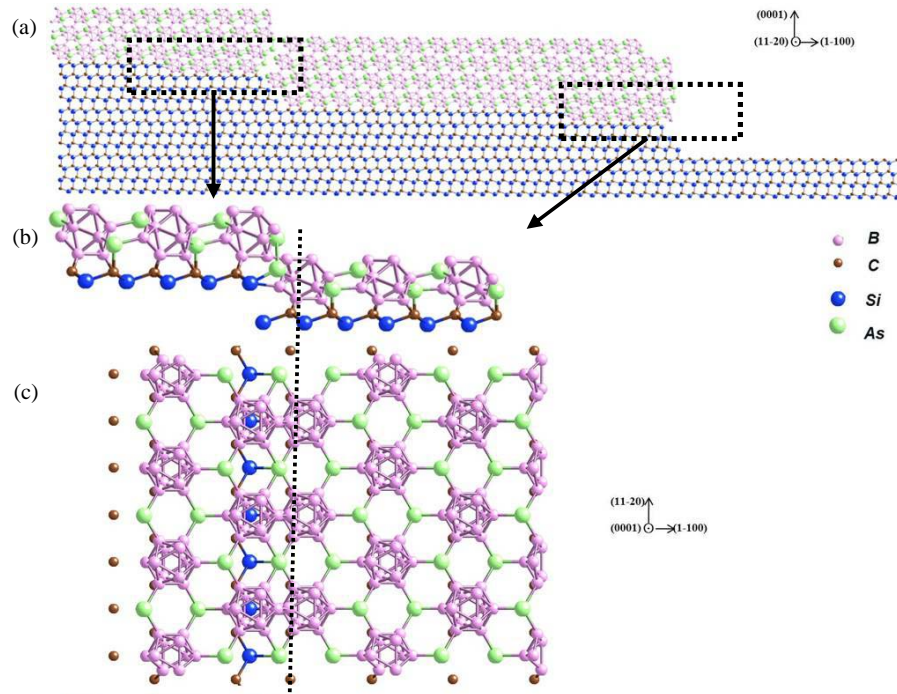

Fig 9 (a) Atomic model of the $B_{12}As_2$/SiC interface showing the nucleation sites; (b) magnified image demonstrating the detailed bonding configurations; (c) plan view of $B_{12}As_2$ nucleated on the surface facets.

only happen for one orientation of the $B_{12}As_2$, which precludes the possibility of rotational domain formation or twins and eliminates the effect of degenerate epitaxy. Nuclei are expected to spread in both directions from such locations and eventually coalesce.

It is shown that the offcut direction of [1-100] in practice interrupts the six-fold symmetry of the c-plane SiC and consequently creates surface morphology with periodic appearance of terraces and adjacent step risers leading to the elimination of degenerate epitaxy.

Evidence for the presence of these step structures was obtained using STEM which

shows an STEM image taking from the interface where a 1/4c step riser is observed (Fig 10(a)) while in Fig 10 (b), a 3/4 unit cell high step riser is observed. Note that only Si and As atoms can be distinguished under STEM.
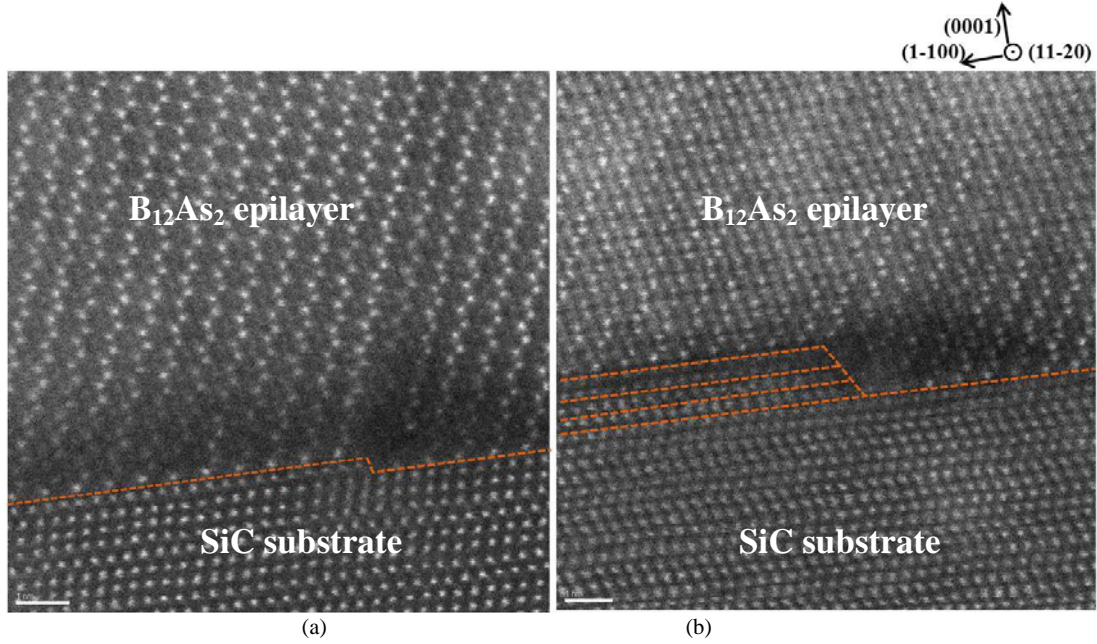

Fig 10 (a) STEM image taking from the interface showing 1/4c unit cell height step riser. (b) STEM image taking from the interface showing 3/4c unit cell height step riser.

The slight diregistry between domains which expand and coalesce from such nucleation sites can lead to the formation of translational domain boundaries while the in-plane mismatch between substrate and the film (~3.7%) can be accommodated by networks of interfacial dislocations.

CONLCUSIONS

Epitaxial growth of $B_{12}As_2$ on c-plane (0001) 4H-SiC substrate both on-axis and with 7° offcut toward [1-100] has been discussed. SWBXT, cross-sectional HRTEM and STEM revealed single crystal, untwinned (111) oriented $B_{12}As_2$ on the latter substrate while twin related domains were found in films grown on on-axis 4H-SiC. It is proposed that the single crystalline, untwinned nature of the $B_{12}As_2$ film resulted from the tendency to nucleate on the isolated junctions between close-packed (-3304) step risers and (0001) terraces present on the

hydrogen etched offcut 4H-SiC surface.

ACKNOWLEDGEMENTS

REFERENCES

[1] S. Bakalova, Y. Gong, C. Cobet, N. Esser, Y. Zhang, J. H. Edgar, Y. Zhang, M. Dudley, and M. Kuball, Phys. Rev. B, 81, 075114 (2010)

[2] G.A. Slack, T.M. McNelly, and E.A. Taft, J. Phys. Chem. Solids, 44, 1009 (1983).

[3] D. Emin, Physics Today, 55, January (1987)

[4] D. Emin, J. Sol. Sta. Chem., 177, 1619 (2004)

[5] M. Carrard, D. Emin and L. Zuppiroli, Phys. Rev. B, 51(17), 11270 (1995).

[6] D. Emin and T. L. Aselage, J. App. Phys., 97, 013529 (2005)

[7] J.R. Michael, T. L. Aselage, D. Emin and P.G. Kotula, J. Mater. Res., 20 (11), 3004 (2005).

[8] D. Emin, J. Sol. Sta. Chem., 179, 2791 (2006)

[9] R.H. Wang, D. Zubia, T. O'Neil, D. Emin, T. Aselage, W. Zhang and S.D. Hersee, J. Electronic Materials, 29 (11), 1304 (2000)

[10] W.M. Vetter, R. Nagarajan, J. H. Edgar and M. Dudley, Mater. Lett., 58, 1331 (2004)

[11] Ordered Boron Arsenide, P. D. Ownby, Journal of the American Ceramic Society, 58, 7-8, 359 (1975)

[12] Y. Gong, M. Tapajna, S, bakalova, Y. Zhang, J. H. Edgar, Y. Zhang, M. Dudley, M. Hopkins and M. Kuball, Appl. Phys. Lett. 96, 223506 (2010).

[13] V. F. Sears, Neutron News 3, 26 (1992).

[14] Z. Xu, J. H. Edgar and S. Speakman, J. Crystal Growth., 293, 162 (2006)

[15] H. Chen, G. Wang, M. Dudley, L. Zhang, L. Wu, Y. Zhu, Z. Xu, J.H. Edgar and M. Kuball,   J. Appl. Phys., 103 (12), 123508 (2008)

[16] J.R. Michael, T.L. Aselage, D. Emin and P.G. Kotula, J. Mater. Res., 20, 3004 (2005)

[17] S.W. Chan, J. Phys. Chem. Solids, 55, 1137 (1994)

[18] C. P. Flynn and J. A. Eades, Thin Soild Films, 389, 116 (2001)

[19] H. Chen, G. Wang, M. Dudley, Z. Xu, J. H. Edgar, T. Batten, M. Kuball, L. Zhang, and Y. Zhu, Appl. Phys. Lett., 92 (23), 231917 (2008)